metals

MDPI

Review

New Insights into the Mechanical Properties, Functional Fatigue, and Structural Fatigue of Ni-Ti Alloy Porous Structures

Dianyu Tang, Yong Hu * and Lei Yang *

School of Transportation and Logistics Engineering, Wuhan University of Technology, Wuhan 430000, China; tdy@whut.edu.cn

* Correspondence: huyong@whut.edu.cn (Y.H.); lei.yang@whut.edu.cn (L.Y.)

Abstract: Ni-Ti shape memory alloys (SMAs) are widely noticed and have captured great interest due to their unique shape memory effect and super elasticity. Porous Ni-Ti SMAs have the typical characteristics of both porous metals as well as shape memory alloys. Because of the uneven stress distribution, cyclic loading has a more significant effect on the phase transformation and plastic deformation of Ni-Ti porous compared with Ni-Ti bulk. This paper overviews the structural and functional fatigue experiments and numerical simulation progress of Ni-Ti porous. The factors affecting the fatigue performance of the Ni-Ti lattice structure and the methods for enhancing its fatigue performance are elaborated. More importantly, the point of the coupling analysis of structural fatigue performance and functional fatigue performance is proposed for the study of porous Ni-Ti shape memory alloys.

Keywords: porous structure; Ni-Ti; shape memory effect; mechanical properties; fatigue

check for updates

Citation: Tang, D.; Hu, Y.; Yang, L. New Insights into the Mechanical Properties, Functional Fatigue, and Structural Fatigue of Ni-Ti Alloy Porous Structures. *Metals* **2023**, *13*, 931. https://doi.org/10.3390/met13050931

Academic Editor: Alexander V. Shelyakov

Received: 2 April 2023
Revised: 27 April 2023
Accepted: 8 May 2023
Published: 10 May 2023

Copyright: © 2023 by the authors. Licensee MDPI, Basel, Switzerland. This article is an open access article distributed under the terms and conditions of the Creative Commons Attribution (CC BY) license (https://creativecommons.org/licenses/by/4.0/).

1. Introduction

Ni-Ti shape memory alloys (SMAs) have an excellent shape memory effect (SME) and super elasticity (SE), which are unique properties that make them promising for applications in aerospace, biomedical and other fields [1]. Thus, the porous structures made by Ni-Ti alloys have an excellent energy absorption capacity, high damping, high specific strength, and biocompatibility while ensuring lightweighting [2,3], which are commonly used for functional parts such as vibration dampers [4], biological bone implants [5], micro-vibration isolators, and smart actuators [6].

Due to the superior damping characteristics and energy absorption capacity, the Ni-Ti porous structures often experience cyclic loading during practical applications. For this reason, fatigue properties have a determining influence on the practical application of Ni-Ti lattice structures [7]. The fatigue behavior of Ni-Ti (SMAs) is mainly divided into functional fatigue and structural fatigue [8,9]. The phenomenon of the shape memory effect and super-elasticity decrease and the residual strain increase during the martensitic cyclic phase transformation of Ni-Ti alloys is known as functional fatigue [10]. An overall fracture failure caused by the sprouting and expansion of cracks when nickel-titanium alloys are cyclically loaded and unloaded is defined as structural fatigue [8,11,12]. Functional fatigue causes dimensional changes, functional deterioration, and even failure of the Ni-Ti lattice structure, while structural fatigue directly induces fracture failure of the part [13].

With the development of manufacturing technology, additive manufacturing technology has breathed new life into Ni-Ti porous structures. The study of Ni-Ti porous structures has shifted from mechanical properties and shape memory properties during loading and offloading to fatigue properties under cyclic loading. Speirs et al. [14] investigated the compressive fatigue behavior of three different cells of SLM Ni-Ti alloy brackets and compared them with conventional octahedral beam structures. Biffi et al. [15] experimentally characterized the lattice structure produced by selective laser melting (SLM) with a nickel-rich

nickel-based alloy as the material. The microstructure, martensitic phase transformation (MT), and hyper-elastic response of the test samples were analyzed and compared with the bulk material.

For studying the fatigue damage mechanism of the Ni-Ti lattice structure, the martensitic cyclic phase transformation model and fatigue damage model are established, and these models are available for the regulation of fatigue performance [16–18]. The development of numerical simulation methods has provided effective methods for solving the aforesaid problems and has proven to be effective in studying fatigue damage mechanisms, which makes it possible to fabricate Ni-Ti lattice structures with predictable properties [19,20]. In recent years, some scholars have focused on the research and development of mechanical response models, martensitic cyclic phase transformation models and fatigue damage models. The porous Ni-Ti structures were designed and prepared by Zhang et al. [21] by the SLM method. A combination of compression experiments and finite element analysis was used to investigate the effect of the compressive behavior of porosity porous Ni-Ti structures. The relationship between the elastic modulus and porosity was established based on the Gibson–Ashby model. The damage mechanism of the porous Ni-Ti structure was analyzed. Ashrafi et al. [17]. developed finite element models at the macroscopic scale to simulate the behavior of Ni-Ti lattice structures fabricated by selective laser melting (SLM). The shape memory properties were investigated by thermodynamic experiments, and appropriate boundary conditions were set for the finite element analysis. Chen et al. [3] investigated the effects of gradient distribution characteristics on the deformation patterns and energy absorption properties of gradient lattice structures (GLS-s) by uniaxial compression tests and finite element analysis. The fracture characteristics of GLS-free, unidirectional GLS, bi-directional increasing GLS, and bi-directional decreasing GLS were analyzed. The common porous structure is shown in Figure 1, along with structural and functional fatigue failure.

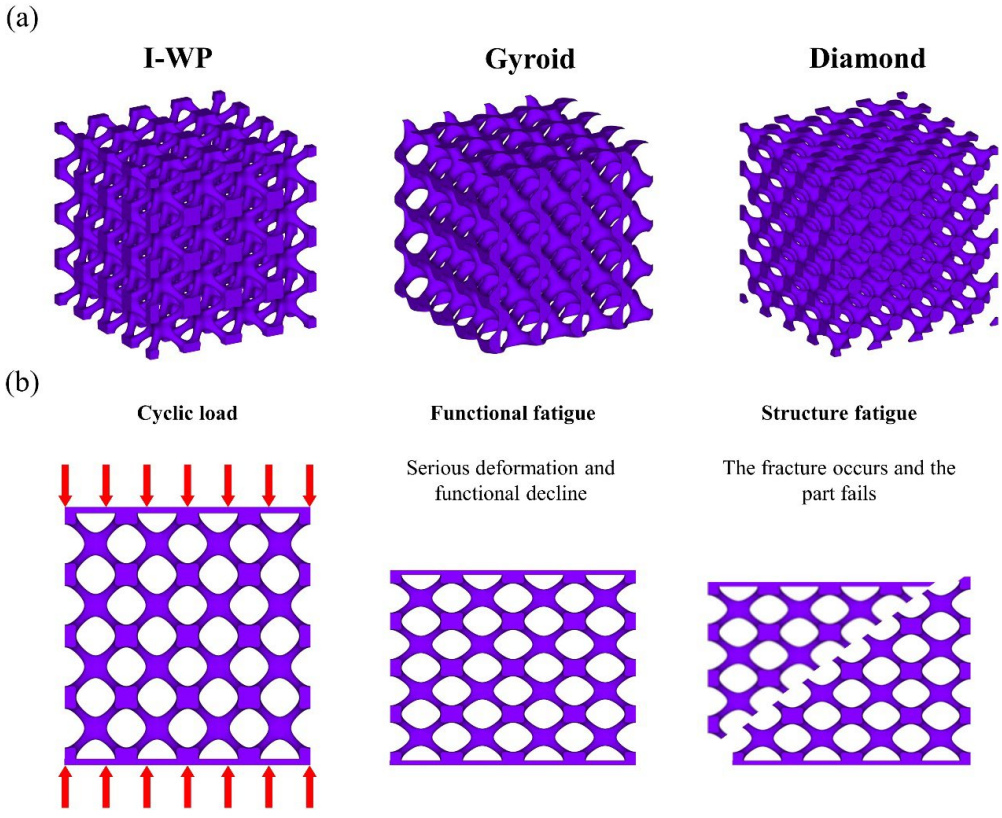


Figure 1. (**a**) Ni-Ti porous structure, (**b**) fatigue failure.

There are few reviews on the fatigue properties of porous nickel-titanium (SMAs). For instance, the progress in enhancing the structural and functional fatigue resistance of Ni-Ti SMAs has been reviewed by Nargatti et al. [22]. Effective parameters for the final properties of Ni-Ti alloys manufactured using powder metallurgy were reviewed by Parvizi et al. [23]. The fatigue behavior of Ni-Ti SMA from low to high cycle (LCF-HCF) was analyzed by Sgambitterra et al. [24]. Zhang et al. reviewed recent advances in AM-Ni-Ti as an orthopedic implant, a porous structure design, and mechanical properties. However, reviews on the functional fatigue and structural fatigue of porous Ni-Ti alloys are rare. Meanwhile, numerical analysis, a popular method for studying mechanical properties in recent years, has not found a summary of the application of numerical simulation in fatigue properties studies.

This paper reviews the latest research and simulation methods for the mechanical, structural fatigue, and functional fatigue properties of Ni-Ti shape memory alloy lattice structures and shows the potential as well as the limitations of different models. The purpose of this review is to provide the readers with a comprehensive analysis of the unique fatigue properties of shape memory alloys and to provide current, reliable, and computationally cost-effective simulation models.

2. Mechanical Response and Structure Fatigue of Ni-Ti Lattice Structures

The excellent mechanical properties of Ni-Ti alloys make them widely available in several industrial fields [25,26]. The mechanical properties of Ni-Ti alloy porous structures and fatigue properties are the focus of current research [27]. Ni-Ti alloys with different structures have different mechanical properties, and many scholars have investigated the mechanical response of different structures in order to improve the performance of Ni-Ti porous structures [28,29].

In order to improve the mechanical and fatigue properties of Ni-Ti porosity, the pore characteristics (porosity, pore shape, and pore size), which tend to cause changes in the mechanical properties, have been investigated [30]. The optimization of manufacturing techniques for Ni-Ti alloy porosity and post-treatment techniques for the manufactured parts have also received attention. The addition of other materials to improve the mechanical properties of porous Ni-Ti has also been studied extensively.

2.1. Influence of Pore Characteristics on the Mechanical Properties of Ni-Ti Porous Structures

At present, several studies have been reported on the factors influencing the mechanical properties of the Ni-Ti lattice structure [31,32]. Lv et al. [30] investigated the effect of different pore strategies on nickel-titanium porous scaffolds at the same porosity. Ni-Ti porous scaffolds with different porosity strategies were prepared by selective laser melting (SLM) based on three-periodic minimal surface (TPMS) structures. A unique conclusion is proposed for the effect of the pore strategy on the microstructure, mechanical properties, and permeability of porous scaffolds. The pore size strategy has a small effect on the mechanical properties of porous scaffolds, and porosity with a continuous gradient distribution positively contributes to the mechanical properties [33]. Figure 2 shows the compressive curves of porous Ni-Ti with different pore sizes, the relationship between the compressive strength and elastic modulus, and the stress–strain curves of compression experiments. In addition, a simulation study was conducted for the permeability analysis of the stent [34].

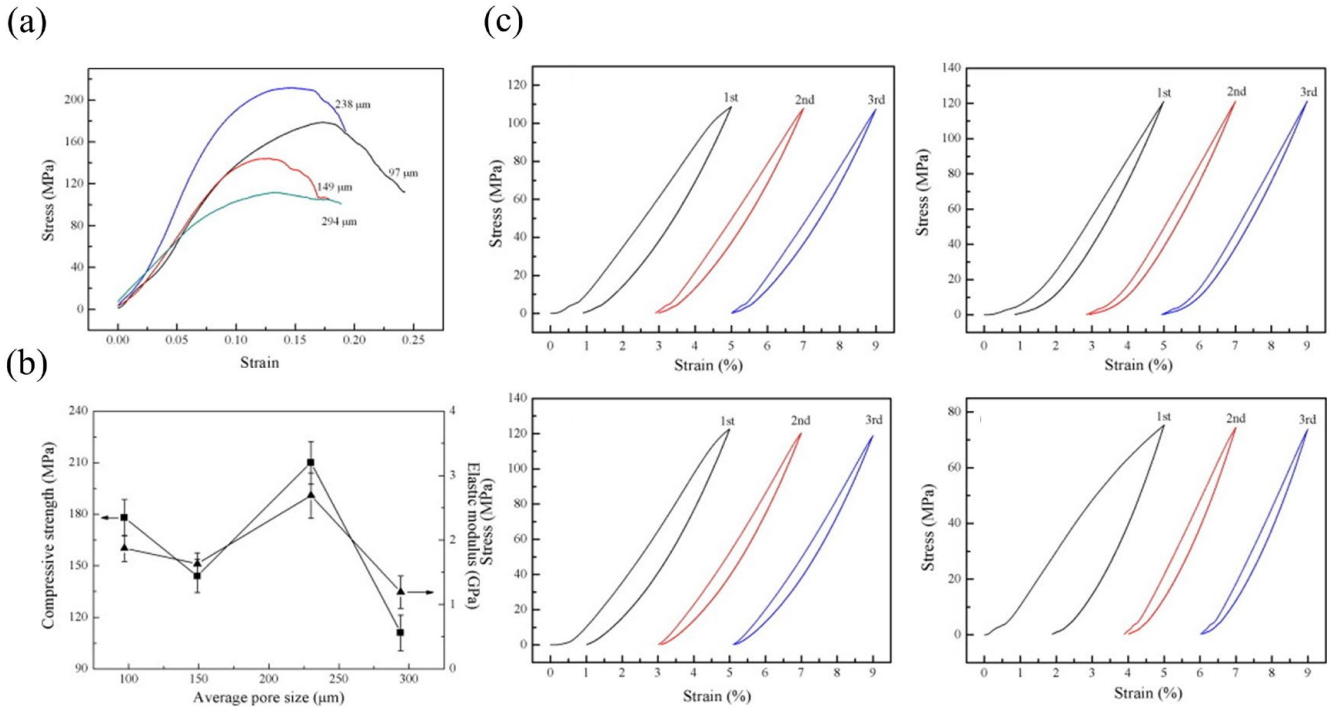


Figure 2. (**a**) Compressive curves of porous Ni-Ti alloys with different pore diameters. (**b**) Relationship between pore diameter and compressive strength and elastic modulus of porous Ni-Ti alloys. (**c**) Stress–strain curves of three loaded-unloaded lap compressive tests at 5% pre-strain for porous Ni-Ti alloys with different pore diameters. Reprinted with permission from Ref. [33]. 2015, Elsevier.

Likewise, Zhang et al. [21] fabricated biomimetic porous Ni-Ti structures with different porosities by SLM. The compression behavior of porous Ni-Ti structures and the failure mechanism were evaluated. Wang et al. [35] prepared porous Ni-Ti alloys by the non-hydrogel gel-casting method and investigated the effect of solid loading upon the microstructure and mechanical properties of the sintered samples. An improvement of the Ni-Ti-SLM method was proposed by Bayati et al. [36] The effect of remelting on the relative density and surface roughness of the parts was investigated. The results revealed that the remelt homogenizes the surface, which allows for the creation of a higher density, fewer defects, and smoother top surfaces. These are important factors that affect the fatigue life and functionality of the parts, and these studies are significant for the future tuning of the mechanical properties of shape memory alloy lattice structures.

2.2. Mechanical Properties of Ni-Ti Porous Structures Influenced by the Preparation Method and Post-Treatment

In some studies, the focus is on optimizing techniques for the preparation of Ni-Ti lattice structures and post-treatment methods [37–39]. Khanlari et al. [40] used the laser powder bed fusion (L-PBF) technique to fabricate dense Ni-Ti alloy parts in three different volume energy densities. The effects of different energy densities and post-treatment on the microstructural properties, phase transformation behavior, and hardness of the samples have been investigated. Wang et al. [41] prepared Ni-Ti nano-porous layers using a dealloying technique. The effect of the de-alloying treatment on the evolution of the organization and mechanical properties of Ni-Ti fibers was investigated, and the weakening mechanism of the nano-porous structures obtained from the de-alloying treatment was discussed. Zhao et al. [42] produced a porous B2-Ni-Ti structure with a fine pore size and uniform pore distribution using a phase leaching process. The method uses a nitric acid solution to etch away the Ni-Gd phase after preparing a Ni-Ti-Ni-Gd duplex pre-alloy with a pore structure. The pore size can be refined by increasing the cooling rate of the pre-alloy.

Post-treatment technology has a significant impact on the mechanical properties of the component. Proper post-treatment can eliminate residual stresses that may arise within the part and reduce the appearance of cracks, further improving the main mechanical properties of the product. As a result, the static properties of the structure as well as the fatigue properties can be enhanced. Porous Ni-Ti alloys with controlled porosity and pore size were prepared with the support of electrically assisted powder metallurgy (EPM) by Ma et al. [43]. Ammonium bicarbonate was used to adjust the porosity and pore size of Ni-Ti alloys and their properties. As shown in Figure 3, the stress–strain curves of the Ni-Ti porous structure under different pre-stress conditions and the residual strain under different porosities are shown. Khanlari et al. [44] fabricated porous 60Ni-Ti parts by conventional pressing and sintering methods. Process parameters were varied in the study to fabricate porous parts with different porosities, and the effects of these processing factors on the microstructure and mechanical properties of porous 60Ni-Ti parts were investigated. The cyclic fatigue characteristics of the samples prepared under the two processes and the cyclic compressive stress–time curves of the samples treated under four different conditions are shown in Figure 4. It was found that treating the parts at a faster heating rate or shorter sintering retention time resulted in sintered and solid solution samples with a lower relative density and higher open volume [45]. By dissolving phases such as Ni3Ti and Ni3Ti2 through solid solution treatment, this heat treatment exhibited higher hardness and approximately the same compressive strength.

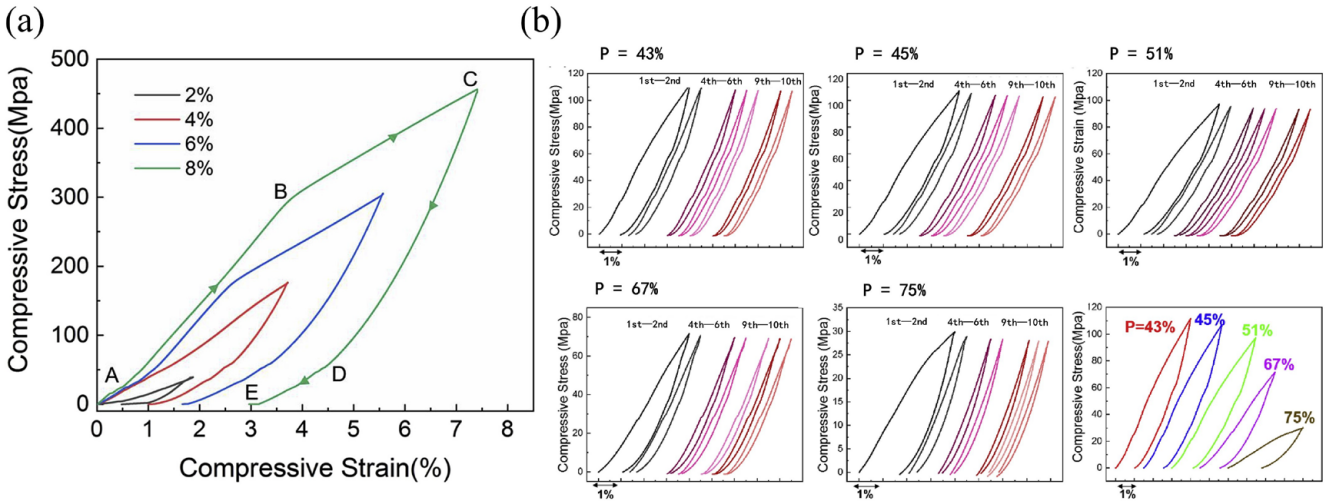


Figure 3. (**a**) Stress–strain curves for loading–unloading compression tests of Ni-Ti alloys under different pre-stresses of 2%, 4%, 6%, and 8%, where section AB corresponds to the austenite elastic deformation phase, section CD is the inverse phase transformation of martensite caused by compressive stress unloading, and section BC is the stress plateau. (**b**) Stress–strain curves for loading–unloading compression tests of porous Ni-Ti with different porosities at 4% pre-strain. Reprinted with permission from Ref. [43]. 2019, Elsevier.

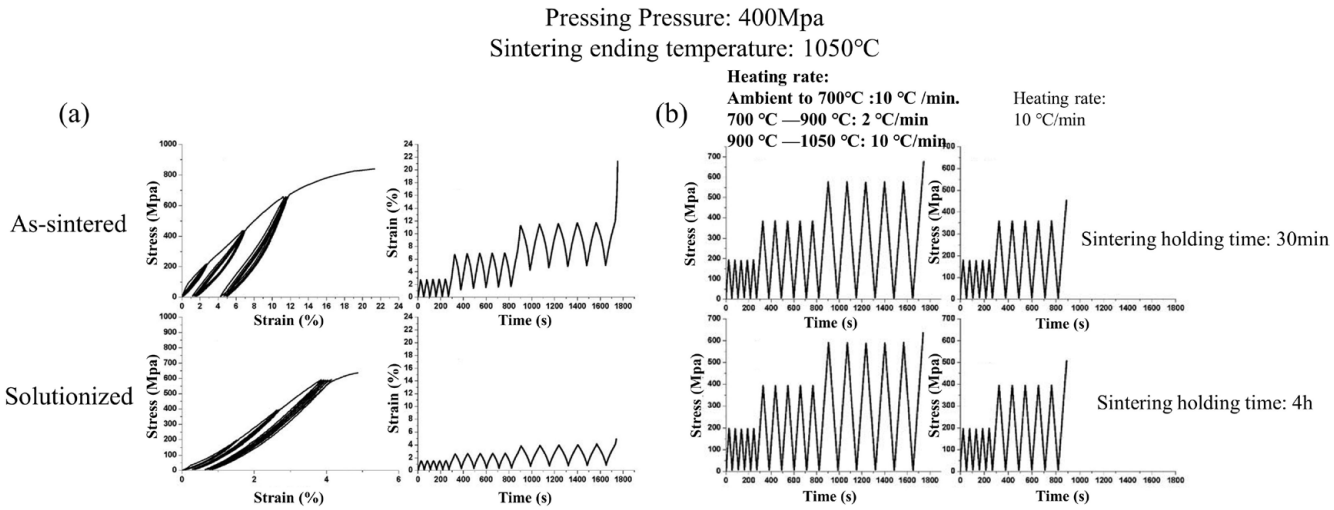


Figure 4. (**a**) Cyclic fatigue characteristics of samples prepared under two processes, (**b**) cyclic compressive stress–time curves of samples treated under four different conditions. Reprinted with permission from Ref. [44]. 2023, Elsevier.

2.3. Mechanical Properties of Ni-Ti Porous Structures Influenced by Additives

Enhancing the mechanical properties of the target structure by adding other materials is one of the most common means. Monogen et al. [46] used self-propagation high-temperature synthesis (SHS) to obtain Ni-Ti porous structures and investigated the effects of aluminum alloying on the macrostructure, microstructure, and mechanical properties of Ni-Ti porous structures. The stress–strain curves of SHS porous Ni-Ti alloys with different aluminum concentrations are shown in Figure 5a. Kaftaranova et al. [47] studied the physical and mechanical properties of porous alloys based on Ni-Ti with different concentrations of Cu additives. The study found that Cu additives enhance the properties of Ni-Ti alloys. The ability of titanium carbide (Ti-C) to enhance the mechanical properties of Ni-Ti composites was investigated by Sharma et al. [48]. Ni-Ti compliant materials reinforced by silver (Ag) infiltration and titanium carbide (Ti-C) were prepared using a powder metallurgical process. In addition, the effect of Ag and Ti-C contents on the microstructure and densification properties of Ni-Ti-Ag-TiC composites was evaluated by field emission scanning electron microscopy (FESEM), energy dispersive spectroscopy (EDS), and X-ray diffraction (XRD).

Anikeev et al. [49] mixed Ni-Ti powder and Ti powder and investigated the structural characteristics of porous materials obtained after sintering with different Ti powder concentrations. It was found that the Ti addition affects the phase formation of the overall Ni-Ti matrix and contributes to the formation of the second phase precipitated as Ti2Ni and Ti3Ni4. These precipitations affect the functional properties of the target material. Abidi et al. [50] prepared porous Ni-Ti shape memory alloys by the pressure-less sintering of NaCl as a spacer under the vacuum condition. The effects of the NaCl powder shape and size on the pore morphology and mechanical properties were investigated. The results showed that the porous alloy with spherical pores showed better mechanical properties compared to the cubic shape. A comparison of the mechanical properties of the porous Ni-Ti with cubic and spherical pores and the fracture samples after compression tests are shown in Figure 5b.

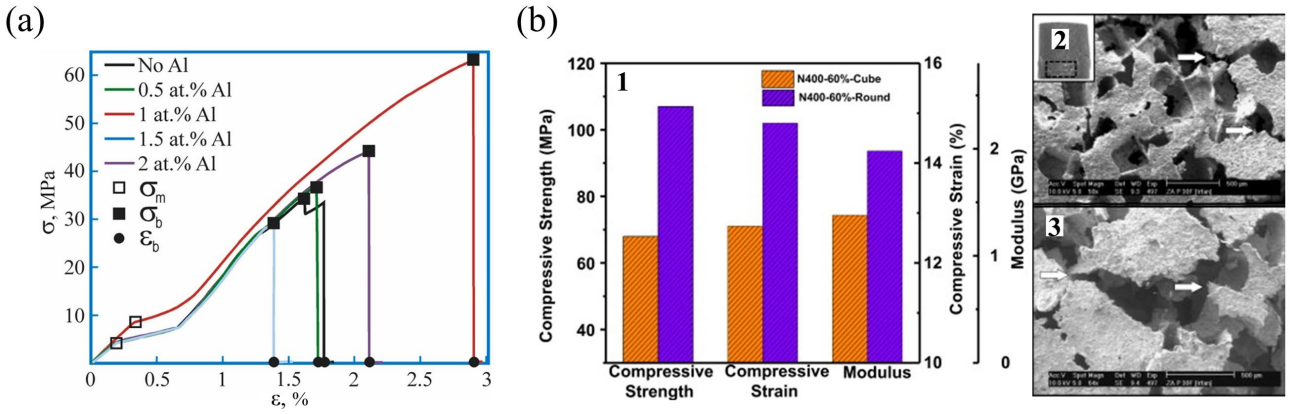


Figure 5. (**a**) Stress–strain curves of SHS porous Ni-Ti alloys with varying Al concentrations. Reprinted with permission from Ref. [46]. 2022, Elsevier (**b**) Comparison of mechanical properties of porous Ni-Ti with cubic and spherical pores and fracture samples after compression tests. (**1**) Bar diagram showing a comparison of mechanical properties of porous Ni-Ti with cubic and spherical pores. (**2**,**3**) Fractured samples after compression test showing crack extension visible through the pore angle. The inset shows the original cylindrical sample after a fracture. Reprinted with permission from Ref. [50]. 2015, Elsevier.

3. Modeling for the Mechanical Response and Structure Fatigue Simulation

One of the most commonly used methods for studying the fatigue and mechanical properties of Ni-Ti alloy lattice structures and even other materials and structures is through various mechanical experiments and fatigue tests. However, the fatigue mechanism of Ni-Ti porous structures is difficult to explain intuitively by experimental studies. Nowadays, numerical simulation techniques have matured, and an increasing number of studies have started to use simulation techniques to explain the fatigue property changes of materials or structures [19,51], such as compression and tension [52].

Mechanical models are often developed in two directions in research; one is mainly used to simulate macroscopic physical behavior such as elastic and plastic behavior, and the other is a reconstruction of the intrinsic model of martensitic phase transformation to investigate the microphysical behavior of the Ni-Ti porous structure [53].

3.1. Macroscopic Ni-Ti Porous Structure Simulation Study

Finite element models with six different levels of porosity were developed by Taheri et al. [54] to simulate the mechanical behavior of porous Ni-Ti with different porosity levels to show the relationship between hardness and porosity levels. The Ni-Ti porous model with different porosity is shown in Figure 6a. Uniaxial compression tests were performed on three samples with different porosity levels to verify the numerical results. The effect of the pore shape on the performance of SMAs was investigated by Liu et al. [55]. The properties of porous SMAs with different porosities and pore shapes were discussed, and the effect of the pore shape on the modulus of porous SMAs and the stress–strain relationship was established. The results show that both Young's modulus and hysteresis decrease with increasing porosity, and the rounder the pores, the better the performance of the material [56]. Zhu et al. [57] developed a three-dimensional constitutive model of SMA by using kinematic hardening theory to modify the Stebner–Brinson (SB) model. Single-hole, double-hole, and array-hole models were developed to simulate elastic deformation, phase transformation, and plastic kinematic hardening behavior, and the modified model with plasticity provided more accurate results. It is shown that there is a complex nonlinear interaction effect between pores rather than a mere superposition. The geometric configuration of the pores is one of the most significant factors affecting the mechanical properties. Ravari et al. [58] used a three-dimensional intrinsic model based on a micro-plane theory that can describe material asymmetry to predict the mechanical response of the cellular

lattice structure. Honeycomb Ni-Ti samples were also fabricated and tested in compression by a selective laser melting process. With these models, the effect of microstructural defects and the asymmetric response of dense SMA on the mechanical properties was investigated, and an effective simulation method was implemented considering the effect of microstructural defects.

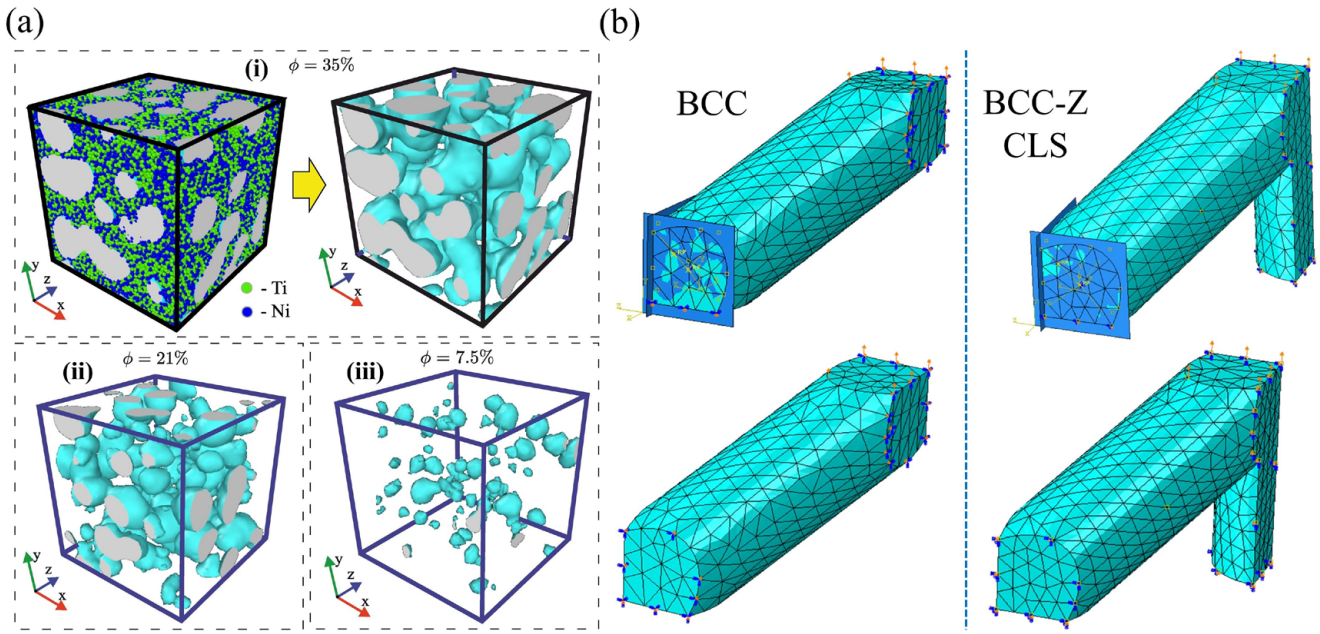


Figure 6. (**a**) Ni-Ti porous model with different porosity, on the left side of panel (**i**), the simulated porous sample is shown. On the right side of panel (**i**) and in panels (**ii**) and (**iii**), a 3D image of the pore wall is shown. Reprinted with permission from Ref. [56]. 2021, Elsevier, (**b**) UUC and MUC models after reduction to a 1/8 model by symmetry; left: BCC and right: BCC-Z CLS. Reprinted with permission from Ref. [17]. 2023, Elsevier.

Ashrafi et al. [17] simulated the behavior of Ni-Ti CLS processed by SLM at the macroscopic scale and developed a new cell model with modified boundary conditions (BC) to predict the Ni-Ti Cellular Lattice Structure (CLS) properties. The UUC and MUC models after reduction to the 1/8 model by symmetry are shown in Figure 6b for the BCC on the left and the BCC-Z CLS on the right. Furthermore, it is noteworthy that the structural model was developed without considering microstructural defects. The BC was modified on the Ni-Ti CLS cell model using finite element analysis based on a modified Souza model using a phenomenological intrinsic model. Finally, the stress–strain model obtained from the finite elements was compared with the experimental curves, showing that the model prediction of the structure has good reliability.

3.2. Microscopic Ni-Ti Porous Structure Simulation Study

Since most of the finite element models (FEM) in past studies have a difficult time directly revealing the actual process of stress-induced martensitic phase transformation (SIM) [59,60], in order to better respond to the mechanical behavior under compression by FEA, Lu et al. [61] reconstructed the intrinsic model of SMA by a new method based on MATLAB image processing to study the mechanical behavior and SIM process and analyzed the mechanical behavior and SIM process on the basis of experiments and simulation. The mechanical behavior and SIM model are discussed on the basis of experimental and simulation analysis. Bagheri et al. [62] extended a microstructure-based multi-stage fatigue (MSF) model to predict the fatigue behavior of AM Ni-Ti subjected to different post-manufacturing heat treatments and compared the predicted fatigue life with experimental specimens. It is important to note that the MSF model can capture the differences in fatigue

behavior under different conditions (process parameters, heat treatment conditions, etc.). This can explain the process–structure–property relationship of the cyclic damage and fatigue life of Ni-Ti alloys more clearly. Allegretti et al. [34] used finite element analysis to assess the fatigue risk and evaluate the fatigue behavior of Ni-Ti brackets through computational modeling and experimental validation. Four strain models were considered: the von Mises criterion and three different damage models (Fatemi–Socie, Brown–Miller, and Simth–Watson–Topper models). However, for multi-axial strains, the accuracy of this model may be limited.

4. Functional Fatigue of Ni-Ti Lattice Structures

The shape memory effect and super-elasticity are the main reasons for the wide application of Ni-Ti shape memory alloys [63,64]. The porous structure of Ni-Ti alloy takes full advantage of its material properties. Due to its operating process, often under cyclic loading, the fatigue performance of Ni-Ti porous structures is a key issue in current research. The fatigue properties of Ni-Ti lattice structures have been studied by many scholars [64–66].

4.1. Pore Characteristics Influence the Functional Fatigue of Ni-Ti Porous Structures

The influence of the pore characteristics of porous structures on their performance is worth investigating. Xu et al. [67] used microwave sintering and space retention techniques for the preparation of porous Ni-Ti alloys with different porosities and pore sizes. The effect of porosity on the mechanical properties as well as the functional fatigue of porous Ni-Ti was investigated. The results show that the strength, as well as super-elasticity of porous Ni-Ti alloys, decreases with increasing porosity. The hyper-elastic recovery strain of porous Ni-Ti reaches between 3.4% and 4.7% when the porosity is 62%. The pore size of porous Ni-Ti depends mainly on the particle size of the occupants. As the pore size of porous Ni-Ti increases, its structural properties show an "S"-shaped trend. When the pore size is less than 294 μm, the super-elasticity of porous Ni-Ti reaches 4% at 5% pre-strain [33]. The cyclic strain curves of porous Ni-Ti with different porosities and the stress–strain curves of cyclic compression tests with different pore sizes at 5% pre-strain are shown in Figure 7a.

Similarly, Zhang et al. [68] developed a process combining discharge plasma sintering (SPS) and space retention techniques in order to prepare porous Ni-Ti alloys. The effect of the pore characteristics and microstructure on the super-elastic behavior of porous Ni-Ti was investigated. The residual and super-elastic recovery strain curves of the porous Ni-Ti alloy at 4% pre-strain are shown in Figure 7d. The effect of pore characteristics on the hyper-elastic reversion strain ratio in a certain range was obtained. The hyper-elastic reversion strain ratio of porous Ni-Ti can reach 90% when the porosity ranges from 18% to 61%, and the average pore size ranges from 21 μm to 415 μm. In the subsequent study, the functionally structurally integrated Ni-Ti porous structure consisting of a central solid and a peripheral porous layer was prepared by SPS. It was found that the obtained Ni-Ti porous obtained a high compressive strength and good hyper-elastic recovery strain (>4%) when the porosity of the inner layer was 14%, that of the outer layer was 49%, and the pore size was controlled to 350 mm [69]. A comparison of the cyclic stress–strain curves of the samples after loading–unloading compression tests with a pre-strain of 4% is shown in Figure 7b. These studies mainly focused on the control of structural properties by changing the pore characteristics.

The relationship between the structural characteristics and reversible shape memory effects of porous Ni-Ti prepared by SHS was investigated by Sergey et al. [70]. The optimization of the structural features was investigated by measuring as well as comparing the multiscale features, martensitic features, and shape memory properties of SHS. Ni-Ti foam structures with porosity in the range of 39–58% were prepared by Nakas et al. [71] by the space scaffold sintering technique. In the study, unidirectional compression and super-elastic cycling at room temperature were used to characterize the mechanical features, and a compression model for Ni-Ti foams with different porosities was proposed. The

hyper-elastic behavior of Ni-Ti foams is explained. It was found that the recovery strain was improved at higher stress levels, and its training period increased when the porosity was below 39%. The response of Ni-Ti foam with 58% porosity and without pre-deformation to applied stress, the dependence of the applied and recovered strain on loading history, and the results of super-elasticity tests are shown in Figure 7c.

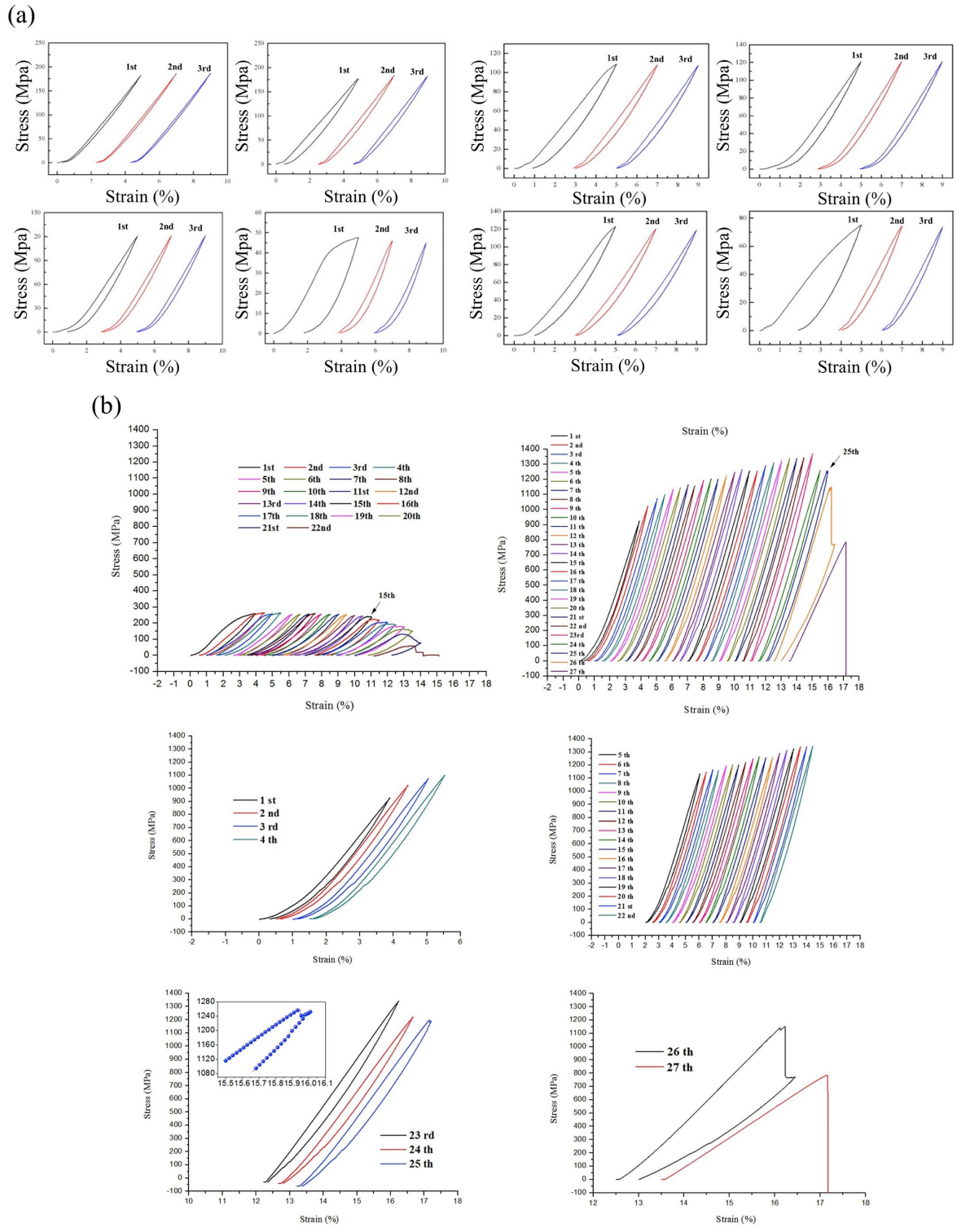


Figure 7. *Cont.*

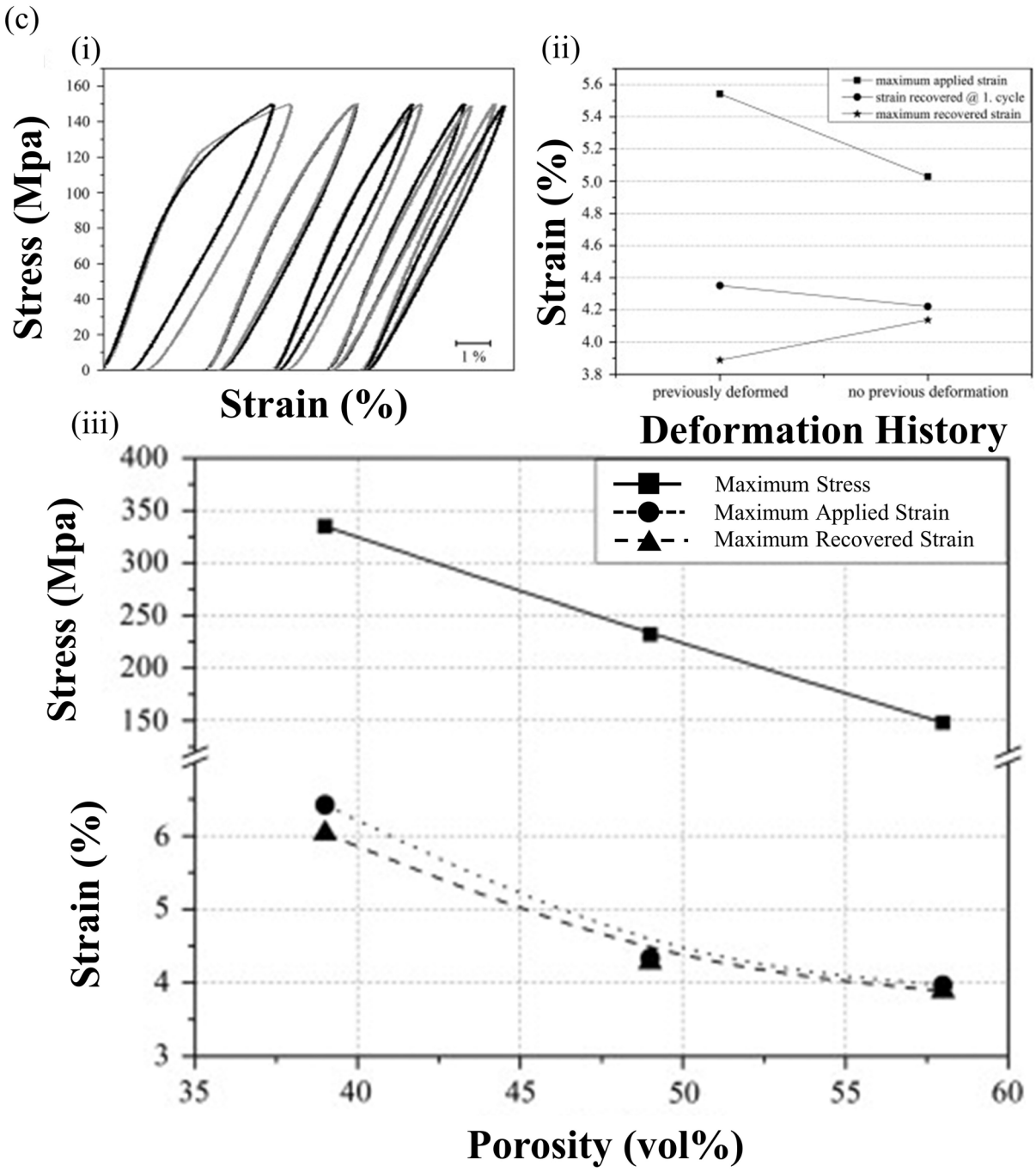


Figure 7. *Cont*.

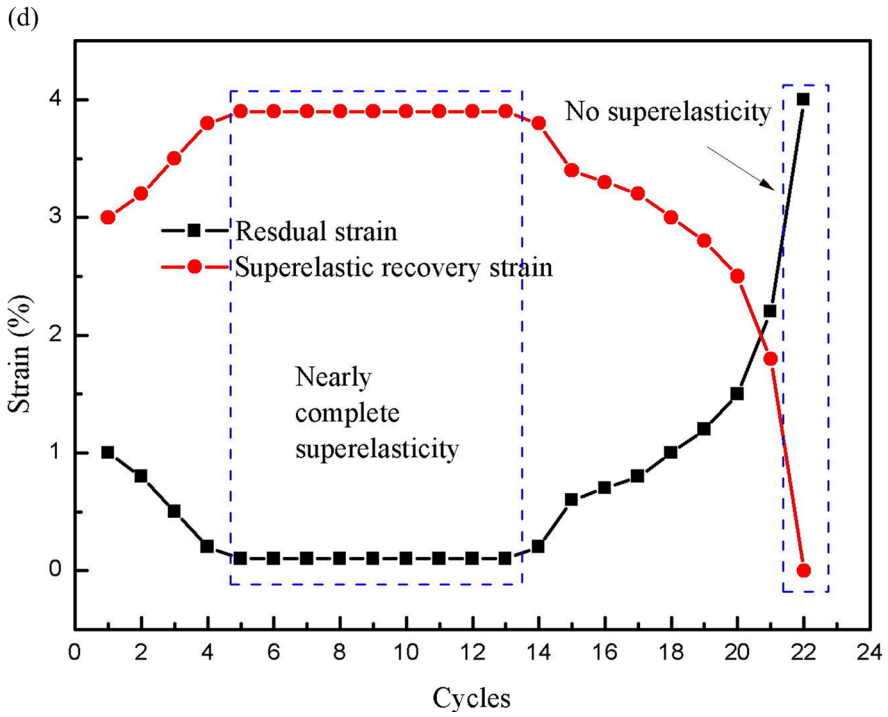


Figure 7. (**a**) Cyclic strain curves for porous Ni-Ti with different porosities and stress–strain curves for cyclic compression tests with different pore sizes at 5% pre-strain; Reprinted with permission from Refs. [33,67]. 2015, Elsevier. (**b**) Comparison of cyclic stress–strain curves of samples after loading–unloading compression tests with 4% pre-strain; Reprinted with permission from Ref. [69]. 2017, Elsevier, (**c**) (**i**) response of Ti-Ni foam with 58 vol% porosity and no pre-deformation to applied stress, (**ii**) dependence of applied and recovered strains on loading history, and (**iii**) results of hyper-elasticity tests; Reprinted with permission from Ref. [71]. 2013, Elsevier. (**d**) Residual strain and super-elastic recovery strain curves of porous Ni-Ti alloy at 4% pre-strain; Reprinted with permission from Ref. [68]. 2015, Elsevier.

4.2. Impact of Additive Manufacturing on Ni-Ti Porous Structure

Additive manufacturing technology is an advantageous method for preparing porous structural parts of Ni-Ti. Compared with porous structures prepared by conventional methods, the porous structures obtained by additive manufacturing have poor basic mechanical and functional characteristics [1]. Therefore, many studies have been focused on obtaining Ni-Ti porous structures with excellent fatigue properties by improving the preparation process [37,72].

Taheri et al. [73] investigated the mechanical properties and shape memory effects of Ni-Ti porous parts prepared by SLM and prepared Ni-Ti lattice structure samples. The effect of pore morphology on the mechanical response was investigated. Porous Ni-Ti with a good shape memory effect (recovery strain of about 5%) was obtained. The functional stability and the mechanical response of the Ni-Ti lattice structure under cyclic loading were evaluated. Chen et al. [3] prepared four gradient lattice structures (GLSs) using the L-PBF technique and combined it with topology optimization. The effects of the gradient distribution on the mechanical properties as well as the functional characteristics of the GLSs were obtained by compression tests and finite element analysis. The shape memory effect of Ni-Ti GLSs prepared by the L-PBF technique was obtained after several compression thermal recovery experiments. It is noteworthy that the study has not separated structural fatigue and functional fatigue but coupled functional fatigue and structural fatigue. Xiong et al. [1] completed the optimization of process parameters for the preparation of Ni-Ti porous structures by micro-laser powder bed (μ-LPBF) melting technology to obtain Ni-Ti micro-components with superior quality and functional properties. The

effects of the processing parameters on the microstructure, phase transition behavior, and mechanical properties of Ni-Ti fabricated by μ-LPBF were revealed, and the mechanical and shape recovery capabilities of Ni-Ti micro-lattice structures and micro-scaffolds were explored. Figure 8 demonstrates the compressive and shape recovery properties of Ni-Ti micro-lattices and micro-scaffolds fabricated by μ-LPBF.

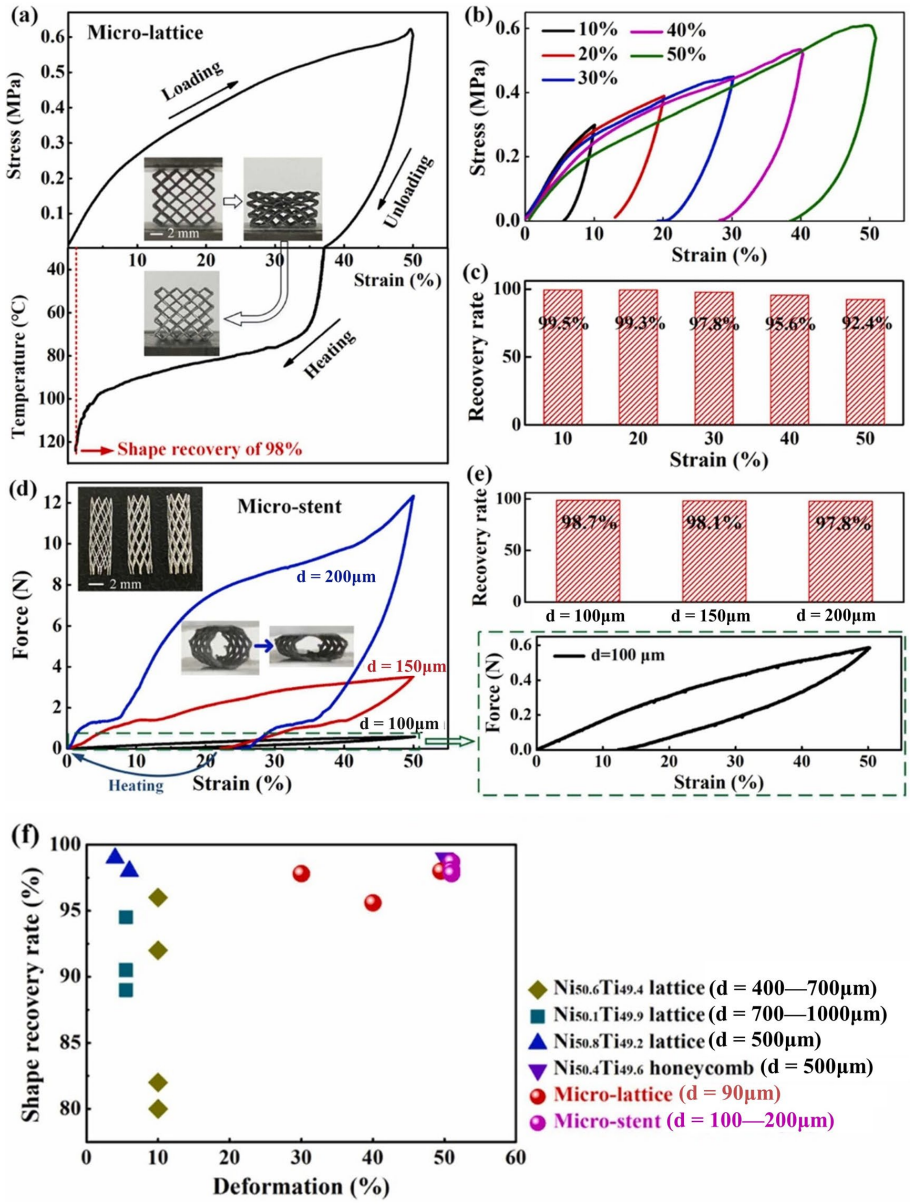


Figure 8. (**a**) Loading-unloading-heating curves of Ni-Ti micro-lattice at 50% compressive strain. The inset shows the images of the micro-lattice before and after deformation and after recovery from heating. (**b**) Cyclic stress-strain curves of Ni-Ti micro-lattice for a gradual increase of compressive strain from 10% to 50%. (**c**) Shape recovery rate of Ni-Ti micro-lattice versus compressive strain during cycling. (**d**) Force-strain curves of Ni-Ti microscopic scaffolds with different strut diameters. The inset is an image of the fabricated sample and screenshots of the compression process. The green dashed box on the right shows a magnification of the curve for a microscopic scaffold with a strut diameter of 100 μm. (**e**) Shape memory rate of Ni-Ti micro-scaffolds with different strut diameters. (**f**) Shape recovery rate and deformable strain of our μ-LPBF fabricated Ni-Ti micro-lattice/scaffold compared to the reported LPBF fabricated Ni-Ti structures. Reprinted with permission from Ref. [1]. 2022, Elsevier.

5. Modeling for the Functional Fatigue Simulation

Porous shape memory alloys combine the advantages of shape memory alloys such as super elasticity and shape memory effect. The computational micromechanical analysis of porous SMAs using finite element methods has become one of the most common methods [74,75]. Currently, fewer studies have been conducted on the functional fatigue simulation of Ni-Ti porosity, and most of them have evaluated the shape memory properties in a single pass [16,76,77], with less research on the super-elasticity under cyclic loading and the shape memory effect [18,78]. Current research focuses on the influence of the pore shape on the super-elasticity and shape memory effects.

Zhu et al. [79] proposed a model based on the Gurson–Tvergaard–Needleman (GTN) model that can reproduce the hyper-elasticity, tensile-compression asymmetry, and internal cycling of porous SMAs under combined loading. The model was compared with the finite element results in the literature for model validation in the study. Yu et al. [80] used finite element techniques by analyzing the shape recovery performance of four bionic lattice structure models. The results show that their selected bionic lattice models have a shape recovery rate of 99% after being subjected to compressive strain. The high shape recovery capability was also achieved under high deformation. Ma et al. [81] evaluated the effect of pore channel properties on the structural hyper-elasticity of helical porous structures (HPS) prepared by SLM. Unsuitable process parameters during SLM processing can result in the appearance of metallurgical pores, which will negatively affect mechanical properties. Therefore, a new strategy is proposed to construct the porous structure of the component by metallurgical pores, and the effect of different metallurgical pore morphologies on the hyper-elasticity of the porous Ni-Ti structure is evaluated to explain the deformation behavior of the metallurgical pores. Analyzing the experimental and simulation results, it is found that the stress concentration occurring near the pores leads to higher residual strain and thus the deterioration of hyper-elasticity as well as mechanical property failure.

A microstructural model for simulating the functional mechanical properties of Ni-Ti porous structures was proposed by Volkov et al. [82]. The model can describe the super-elasticity, deformation plasticity, and shape memory effects of SMA and explains the strain accumulation during cooling and the reverse strain during the heating of the specimen when under constant compressive stress. Shariat et al. [83] simulated the typical hysteresis elastic mechanical behavior of Ni-Ti orifice plates using a finite element method. The model decomposes the mechanical response of Ni-Ti into hyper-elastic as well as hysteretic stresses. The hyper-elastic and hysteretic stresses describe the reversible as well as the irreversible aspects of the process. In addition, the pseudo-elastic deformation behavior of Ni-Ti plates with through-holes is also discussed. The effect of hole morphology on the stress–strain behavior is discussed by a numerical model based on the elasto-plastic model. An increase in the diameter of the hole promotes the range of stress gradients and suppresses the stress plateau. Better controllability is provided for shape memory components when the gradient stress exceeds the phase transition stress. Finally, numerical results are compared and validated with experimental data [84]. The modeling and simulation of a four-hole bone fixation plate were completed by Jahadakbar et al. [76], and fixed plates with different porosities were designed using the AM technique and tested mechanically under tension. Maitrejean et al. [85] used representative volume elements (RVE) and scaling relations to describe the hyper-elastic behavior of porous SMAs. This approach does not require a conventional porous microstructure model and can substantially reduce the computational cost.

6. Application of Ni-Ti Porous Structure

The unique properties of Ni-Ti alloys, such as shape memory (or pseudo-elasticity) and super-elasticity, have garnered significant interest. The shape memory properties allow Ni-Ti alloys to recover their original shape even after significant deformation thanks to the reversible martensitic transformation of their crystal structure. Moreover, Ni-Ti alloys exhibit super-elasticity, which enables them to withstand high loads without permanent

deformation or mechanical failure [86]. Combining these properties with a porous structure makes porous Ni-Ti particularly promising in the fields of medical devices, aerospace engineering, and structural materials [42], as it can offer the advantages of both porous materials and shape memory alloys.

For instance, porous Ni-Ti alloys have been widely used in biomedical applications [26,87]. First, Ni-Ti alloys have good mechanical properties, biocompatibility, and corrosion resistance, making them a promising biomaterial for bone implantation. In addition, their porous structure provides a favorable environment for cell growth and transport, leading to effective osseointegration and integration with surrounding tissues. Aihara et al. [25] used combustion synthesis (CS) to produce the porous Ni-Ti alloy and evaluated its potential as a bone implant material. The study showed that bone tissue integrated rapidly into the porous structure within two weeks, indicating high biocompatibility and osseointegration properties. These observed properties of porous Ni-Ti alloys have the potential to accelerate the healing process and improve long-term stability, making them a promising material for bone implant applications. Zhou et al. [88] fabricated the porous Ni-Ti shape memory alloy (SMA) with graded porosity, inspired by human long bones. Their study demonstrated that the mechanical properties of this material are more similar to those of human long bones, potentially extending the application range of Ni-Ti SMA with graded porosity. Zhang et al. [89] employed finite element simulations to evaluate the potential use of Menger sponge fractal Ni-Ti structures as bone implants. Their study showed that by adjusting the porosity and fractal parameters of the structure to match the porosity characteristics of bone, the Menger sponge fractal structure holds great potential for bone implantation. The pore characteristics of porous Ni-Ti alloys play a key role in their practical applications. Specifically, the pore size of the material influences the available space for cell proliferation and directly affects the growth and development of cellular tissue within the implant [90]. Figure 9a displays scanning electron microscopy (SEM) images of MC3T3-E1 cells on Ni-Ti samples, which were cultured in a humid environment at 37 °C. Jian et al. [91] conducted a study in which they prepared five different porous Ni-Ti samples with varying pore characteristics. The cytocompatibility experiments were then performed to investigate the effect of these pore characteristics on the mechanical and biological properties of the material. Liu et al. [92] determined the hyper-elastic biomechanical properties of porous Ni-Ti scaffolds and evaluated their impact on bone growth in vivo. The results showed that capsule-free thermoisostatic pressing (CF-HIP) synthesized Ni-Ti promotes bone growth. The morphology of osteoblasts on various surfaces of porous Ni-Ti scaffolds is illustrated in Figure 9b. Further investigation into the pore characteristics of porous Ni-Ti for use in implants is warranted.

The use of porous Ni-Ti alloys has mainly been focused on biomedicine, but there is still potential for them to be used in aerospace and structural materials as well [93,94]. In a study by Zhao et al. [42], a phase leaching process was used to create B2-Ni-Ti compounds with finely distributed pores. The researchers found that reducing the porosity of these alloys could improve their mechanical and damping properties. This suggests that fine-porous Ni-Ti alloys with uniform characteristics could be used as damping materials in various engineering applications.

Another study conducted by Kakaei et al. [95] investigated the electrochemical response of porous Ni-Ti nanostructures in terms of energy storage and corrosion protection. The capacitance of partially oxidized Ni-Ti alloys was measured at different current densities to evaluate their charge transfer capabilities. The findings showed that partially oxidized Ni-Ti can be used as a capacitive material for supercapacitors in alkaline and sodium sulfate solutions. This research highlights the potential of porous Ni-Ti in energy storage applications.

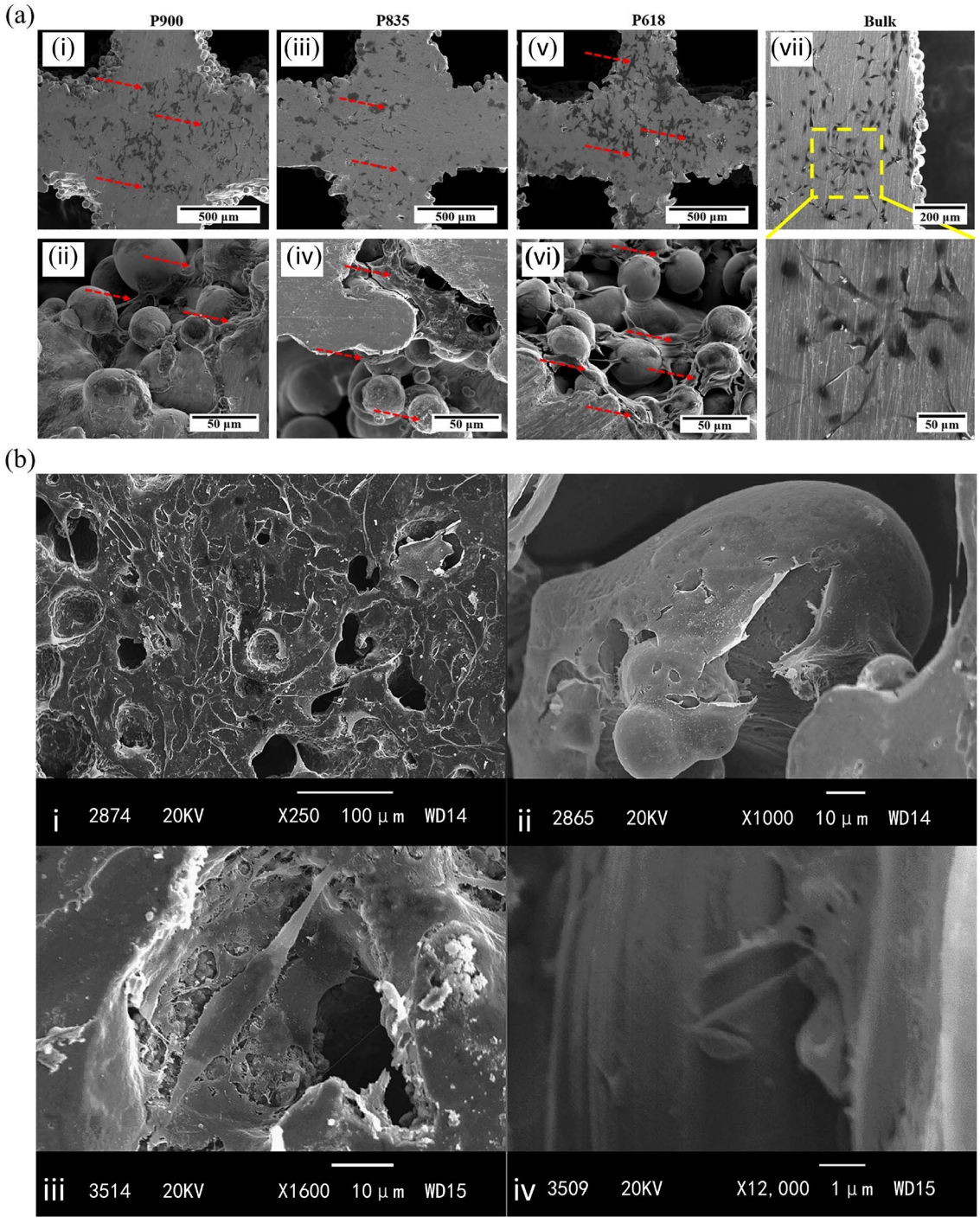


Figure 9. (**a**) SEM images of MC3T3-E1 cells on NiTi samples after 7 days of culture in a humid environment at 37 °C. MC3T3E1 cells on the outer surface of the porous NiTi stent (**i**,**iii**,**v**) and on the inner surface of (**ii**,**iv**,**vi**), and (**vii**) MC3T3-E1 cells on the bulk NiTi samples. Reprinted with permission from Ref. [90]. 2021, Elsevier. (**b**) SEM images showing osteoblast morphology on different surfaces of porous NiTi scaffolds: (**i**) spreading over the entire surface, (**ii**) growing on convex surfaces, (**iii**) growing on exposed pore surfaces, and (**iv**) invading into internal pores along interconnected channels. Reprinted with permission from Ref. [92]. 2011, Elsevier.

Moreover, Bewerse et al. [96] utilized a powder metallurgical technique that involved using steel wire as a spatial scaffold to produce Ni-Ti porous structures with fully interconnected three-dimensional microchannels. This method allows for precise control over

the volume fraction of the microchannels. The researchers observed that the optimized treatment resulted in shape memory properties, making the structure highly suitable for energy absorption or actuator applications. This study emphasizes the potential of this approach for developing innovative porous Ni-Ti structures with customized properties. Nonetheless, further research is necessary to fully explore and expand the potential of these materials in these fields.

7. Summaries and Perspectives

More and more scholars have become interested in additive manufacturing processes in recent years, and metal additive manufacturing has unique advantages over other techniques in preparing complex parts with high dimensional accuracy. The topological parameters of SMA complex structures can be precisely controlled to modulate the mechanical properties as well as the shape memory properties.

Currently, the factors influencing the fatigue performance of Ni-Ti porous structures are receiving most of the attention—for example, the enhancement or decaying effects of pore properties (porosity, pore shape, pore size, etc.) on structural and functional fatigue. With the maturity of additive manufacturing technology, many researchers have investigated various methods of forming porous Ni-Ti and compared the impact of different forming methods and different process parameters on the mechanical properties of porous Ni-Ti. However, the current research objects are mostly truss-type porous structures obtained from simple geometric units by Boolean operations. Under the influence of additive manufacturing technology, these structures are simple to be formed, but local stress concentrations are highly likely to occur, and the local stress concentrations and damage need to be paid attention to due to the unstable forming quality. In addition, porous Ni-Ti with different topologies can have enhanced structural fatigue as well as functional fatigue properties. In particular, three-cycle minimum surface structures with more uniform load-bearing stress distribution should be the focus of research. The development of different topologies for obtaining the desired mechanical properties will be an important research direction. Some researchers have combined numerical simulations to investigate the mechanical properties of Ni-Ti porous structures in a cost-effective and efficient manner; however, most studies still use simpler models and consider structural and functional properties separately. Therefore, in the direction of Ni-Ti porous fatigue performance simulation, it is worthwhile to study how to establish the internal structural damage mechanism as well as the functional decay mechanism.

Functional fatigue and structure fatigue should not be studied separately. Martensitic phase transformation may form new crack initiation points and also affect the crack expansion rate and path. The local stress concentration and fatigue damage of the Ni-Ti lattice structure cannot be neglected because the quality of additive manufacturing molding is difficult to control. It can be seen that the functional fatigue and structural fatigue of porous Ni-Ti are inseparable and should be coupled and analyzed in order to accurately predict and regulate the fatigue performance of the Ni-Ti lattice structure. The construction of a coupled functional fatigue–structural fatigue intrinsic model for Ni-Ti porous structures is an important direction for the current research on the fatigue performance of porous Ni-Ti.

Author Contributions: Conceptualization, methods, software, writing—original draft preparation, D.T.; validation, formal analysis, investigation, resources, data organization, writing—review and editing, Y.H.; visualization, supervision, project management, funding acquisition, L.Y. All authors have read and agreed to the published version of the manuscript.

Funding: The authors acknowledge the National Natural Science Foundation of China (52105396), the Natural Science Foundation of Hubei Province (No. 2021CFB003), and the Central University Basic Research Funds (No. 2022IVA138) for funding this project.

Data Availability Statement: No new data were created or analyzed in this study. Data sharing is not applicable to this article.

Conflicts of Interest: The authors declare no conflict of interest.

References

1. Xiong, Z.; Li, H.; Yang, H.; Yang, Y.; Liu, Y.; Cui, L.; Li, X.; Masseling, L.; Shen, L.; Hao, S. Micro laser powder bed fusion of NiTi alloys with superior mechanical property and shape recovery function. *Addit. Manuf.* **2022**, *57*, 102960. [CrossRef]
2. Farber, E.; Orlov, A.; Borisov, E.; Repnin, A.; Kuzin, S.; Golubkov, N.; Popovich, A. TiNi Alloy Lattice Structures with Negative Poisson's Ratio: Computer Simulation and Experimental Results. *Metals* **2022**, *12*, 1476. [CrossRef]
3. Chen, W.; Gu, D.; Yang, J.; Yang, Q.; Chen, J.; Shen, X. Compressive mechanical properties and shape memory effect of NiTi gradient lattice structures fabricated by laser powder bed fusion. *Int. J. Extrem. Manuf.* **2022**, *4*, ac8ef3. [CrossRef]
4. Zhang, M.; Yu, Q.; Liu, Z.; Zhang, J.; Tan, G.; Jiao, D.; Zhu, W.; Li, S.; Zhang, Z.; Yang, R. 3D printed Mg-NiTi interpenetrating-phase composites with high strength, damping capacity, and energy absorption efficiency. *Sci. Adv.* **2020**, *6*, eaba5581. [CrossRef] [PubMed]
5. Valiev, R.Z.; Prokofiev, E.A.; Kazarinov, N.A.; Raab, G.I.; Minasov, T.B.; Strasky, J. Developing Nanostructured Ti Alloys for Innovative Implantable Medical Devices. *Materials* **2020**, *13*, 967. [CrossRef] [PubMed]
6. Sun, J.; Gu, D.; Lin, K.; Yuan, L.; Yang, J.; Chen, W. Laser powder bed fusion of diatom frustule inspired bionic NiTi lattice structures: Compressive behavior and shape memory effect. *Smart Mater. Struct.* **2022**, *31*, 074003. [CrossRef]
7. Mirak, M.; Alizadeh, M.; Salahinejad, E.; Amini, R. Zn-HA-TiO_2 nanocomposite coatings electrodeposited on a NiTi shape memory alloy. *Surf. Interface Anal.* **2015**, *47*, 176–183. [CrossRef]
8. Frenzel, J. On the Importance of Structural and Functional Fatigue in Shape Memory Technology. *Shape Mem. Superelast.* **2020**, *6*, 213–222. [CrossRef]
9. Luo, J.; Yarigarravesh, M.; Assari, A.H.; Amin, N.H.; Tayyebi, M.; Paidar, M. Investigating the solid-state diffusion at the interface of Ni/Ti laminated composite. *J. Manuf. Process.* **2022**, *75*, 670–681. [CrossRef]
10. Gao, Y.; Yu, T.; Wang, Y. Phase Transformation Graph and Transformation Pathway Engineering for Shape Memory Alloys. *Shape Mem. Superelast.* **2020**, *6*, 115–130. [CrossRef]
11. Ye, Q.; Li, X.; Tayyebi, M.; Assari, A.H.; Polkowska, A.; Lech, S.; Polkowski, W.; Tayebi, M. Effect of heat treatment parameters on microstructure evolution, tensile strength, wear resistance, and fracture behavior of Ni–Ti multilayered composites produced by cross-accumulative roll bonding. *Arch. Civ. Mech. Eng.* **2022**, *23*, 27. [CrossRef]
12. Amini, R.; Alijani, F.; Ghaffari, M.; Alizadeh, M.; Okyay, A.K. Formation of B19′, B2, and amorphous phases during mechano-synthesis of nanocrystalline NiTi intermetallics. *Powder Technol.* **2014**, *253*, 797–802. [CrossRef]
13. Hosseini, S.; Karimidoost, M.; Emamian, M.; Mehrjoo, M.; Alishahi, M. Electrochemical dealloying of porous NiTi alloy: Porosity evolution, corrosion resistance, and biocompatibility behavior. *Intermetallics* **2023**, *152*, 107756. [CrossRef]
14. Speirs, M.; Van Hooreweder, B.; Van Humbeeck, J.; Kruth, J.P. Fatigue behaviour of NiTi shape memory alloy scaffolds produced by SLM, a unit cell design comparison. *J. Mech. Behav. Biomed. Mater.* **2017**, *70*, 53–59. [CrossRef]
15. Biffi, C.A.; Bassani, P.; Fiocchi, J.; Tuissi, A. Microstructural and Mechanical Response of NiTi Lattice 3D Structure Produced by Selective Laser Melting. *Metals* **2020**, *10*, 814. [CrossRef]
16. Zhao, M.; Qing, H.; Wang, Y.; Liang, J.; Zhao, M.; Geng, Y.; Liang, J.; Lu, B. Superelastic behaviors of additively manufactured porous NiTi shape memory alloys designed with Menger sponge-like fractal structures. *Mater. Des.* **2021**, *200*, 109448. [CrossRef]
17. Ashrafi, M.J.; Amerinatanzi, A.; Saebi, Z.; Shayesteh Moghaddam, N.; Mehrabi, R.; Karaca, H.; Elahinia, M. Shape memory response of cellular lattice structures: Unit cell finite element prediction. *Mech. Mater.* **2018**, *125*, 26–34. [CrossRef]
18. Saedi, S.; Saghaian, S.E.; Jahadakbar, A.; Shayesteh Moghaddam, N.; Taheri Andani, M.; Saghaian, S.M.; Lu, Y.C.; Elahinia, M.; Karaca, H.E. Shape memory response of porous NiTi shape memory alloys fabricated by selective laser melting. *J. Mater. Sci. Mater. Med.* **2018**, *29*, 40. [CrossRef]
19. He, X.; Tong, Z.; Du, H.; Wang, D.; Wang, L.; Melnik, R. Modeling microstructure evolution in shape memory alloy rods via Legendre wavelets collocation method. *J. Mater. Sci.* **2019**, *54*, 14400–14413. [CrossRef]
20. Tsouknidas, A.; Michailidis, N.; Maliaris, G.; Makkar, J.; Baxevanis, T.; Lagoudas, D. A numerical study of "functional fatigue" of closed-cell NiTi shape memory foams. *Mech. Mater.* **2019**, *131*, 11–21. [CrossRef]
21. Zhang, X.; Jiang, Y.; Wang, S.; Wang, S.; Wang, Z.; Yu, Z.; Zhang, Z.; Ren, L. Compression Behavior and Failure Mechanisms of Bionic Porous NiTi Structures Built via Selective Laser Melting. In *Acta Metallurgica Sinica (English Letters)*; Springer: Berlin/Heidelberg, Germany, 2023.
22. Nargatti, K.; Ahankari, S. Advances in enhancing structural and functional fatigue resistance of superelastic NiTi shape memory alloy: A Review. *J. Intell. Mater. Syst. Struct.* **2021**, *33*, 503–531. [CrossRef]
23. Parvizi, S.; Hashemi, S.M.; Asgarinia, F.; Nematollahi, M.; Elahinia, M. Effective parameters on the final properties of NiTi-based alloys manufactured by powder metallurgy methods: A review. *Prog. Mater. Sci.* **2021**, *117*, 100739. [CrossRef]
24. Sgambitterra, E.; Magarò, P.; Niccoli, F.; Renzo, D.; Maletta, C. Novel insight into the strain-life fatigue properties of pseudoelastic NiTi shape memory alloys. *Smart Mater. Struct.* **2019**, *28*, ab3df1. [CrossRef]
25. Aihara, H.; Zider, J.; Fanton, G.; Duerig, T. Combustion Synthesis Porous Nitinol for Biomedical Applications. *Int. J. Biomater.* **2019**, *2019*, 4307461. [CrossRef]
26. Li, Y.-H.; Li, J.-H. NiTi/PMMA Biocomposite: In Situ Polymerization, Microstructure and Mechanical Property. *Trans. Indian Inst. Met.* **2022**, *76*, 945–950. [CrossRef]
27. Panton, B.; Michael, A.; Zhou, Y.N.; Khan, M.I. Effects of post-processing on the thermomechanical fatigue properties of laser modified NiTi. *Int. J. Fatigue* **2019**, *118*, 307–315. [CrossRef]

28. Zhao, C.; Liang, H.; Luo, S.; Yang, J.; Wang, Z. The effect of energy input on reaction, phase transition and shape memory effect of NiTi alloy by selective laser melting. *J. Alloy. Compd.* **2020**, *817*, 153288. [CrossRef]
29. Zhang, D.; Hu, Z.; Li, Y.; Cong, W. Excellent damping properties and their correlations with the microstructures in the NiTi alloys fabricated by laser-directed energy deposition. *J. Manuf. Process.* **2022**, *84*, 965–976. [CrossRef]
30. Lv, Y.; Liu, G.; Wang, B.; Tang, Y.; Lin, Z.; Liu, J.; Wei, G.; Wang, L. Pore Strategy Design of a Novel NiTi-Nb Biomedical Porous Scaffold Based on a Triply Periodic Minimal Surface. *Front. Bioeng. Biotechnol.* **2022**, *10*, 910475. [CrossRef]
31. Marchenko, E.; Baigonakova, G.; Shishelova, A. Influence of the Gas Reaction Atmosphere on the Structure, Phase Composition, Functional Properties and Cytocompatibility of Porous Titanium–Nickel Alloys. *Metals* **2022**, *12*, 2170. [CrossRef]
32. Hosseini, S.A.; Yazdani-Rad, R.; Kazemzadeh, A.; Alizadeh, M. A Comparative Study on the Mechanical Behavior of Porous Titanium and NiTi Produced by a Space Holder Technique. *J. Mater. Eng. Perform.* **2013**, *23*, 799–808. [CrossRef]
33. Xu, J.L.; Bao, L.Z.; Liu, A.H.; Jin, X.F.; Luo, J.M.; Zhong, Z.C.; Zheng, Y.F. Effect of pore sizes on the microstructure and properties of the biomedical porous NiTi alloys prepared by microwave sintering. *J. Alloy. Compd.* **2015**, *645*, 137–142. [CrossRef]
34. Allegretti, D.; Berti, F.; Migliavacca, F.; Pennati, G.; Petrini, L. Fatigue Assessment of Nickel–Titanium Peripheral Stents: Comparison of Multi-Axial Fatigue Models. *Shape Mem. Superelast.* **2018**, *4*, 186–196. [CrossRef]
35. Wang, Z.; He, Z.; Duan, B.; Liu, X.; Wang, D. Influence of Solid Loading on the Gel-Casting of Porous NiTi Alloys. *Materials* **2022**, *15*, 8398. [CrossRef]
36. Bayati, P.; Safaei, K.; Nematollahi, M.; Jahadakbar, A.; Yadollahi, A.; Mahtabi, M.; Elahinia, M. Toward understanding the effect of remelting on the additively manufactured NiTi. *Int. J. Adv. Manuf. Technol.* **2020**, *112*, 347–360. [CrossRef]
37. Wan, X.; Feng, Y.; Lin, X.; Tan, H. Large superelastic recovery and elastocaloric effect in as-deposited additive manufactured $Ni_{50.8}Ti_{49.2}$ alloy. *Appl. Phys. Lett.* **2019**, *114*, 221903. [CrossRef]
38. Tan, C.; Zou, J.; Li, S.; Jamshidi, P.; Abena, A.; Forsey, A.; Moat, R.J.; Essa, K.; Wang, M.; Zhou, K.; et al. Additive manufacturing of bio-inspired multi-scale hierarchically strengthened lattice structures. *Int. J. Mach. Tools Manuf.* **2021**, *167*, 103764. [CrossRef]
39. de Wild, M.; Schollbach, T.; Schumacher, R.; Schkommodau, E.; Bormann, T. Effects of laser parameters and scanning strategy on structural and mechanical properties of 3D NiTi implants fabricated with selective laser melting. *Biomed. Eng. Biomed. Tech.* **2013**, *58* (Suppl. S1), 000010151520134088. [CrossRef]
40. Khanlari, K.; Shi, Q.; Li, K.; Hu, K.; Cao, P.; Liu, X. Effects of printing volumetric energy densities and post-processing treatments on the microstructural properties, phase transformation temperatures and hardness of near-equiatomic NiTinol parts fabricated by a laser powder bed fusion technique. *Intermetallics* **2021**, *131*, 107088. [CrossRef]
41. Wang, H.; Wang, B.; Liu, Z.; Zhao, J.; Zhang, H. Microstructure and mechanical properties of NiTi nanoporous structures fabricated with dealloying process. *J. Alloy. Compd.* **2023**, *933*, 167804. [CrossRef]
42. Zhao, M.; Shao, Y.; Zheng, W.; Luo, Y.; Qiao, J.; Wu, S.; Yan, Y.; Guo, W. Tailoring the damping and mechanical properties of porous NiTi by a phase leaching process. *J. Alloy. Compd.* **2021**, *855*, 157471. [CrossRef]
43. Ma, X.; Wang, H.; Xie, H.; Qu, J.; Chen, X.; Chen, F.; Song, Q.; Yin, H. Engineering the porosity and superelastic behaviors of NiTi alloys prepared by an electro-assisted powder metallurgical route in molten salts. *J. Alloy. Compd.* **2019**, *794*, 455–464. [CrossRef]
44. Khanlari, K.; Ramezani, M.; Kelly, P.; Cao, P.; Neitzert, T. Mechanical and microstructural characteristics of as-sintered and solutionized porous 60NiTi. *Intermetallics* **2018**, *100*, 32–43. [CrossRef]
45. Liu, B.; Liu, Z.; Liu, X.; Wang, W.; Wang, L. Effect of sintering temperature on the microstructure and mechanical properties of $Ti_{50}Ni_{50}$ and $Ti_{47}Ni_{47}Al_6$ intermetallic alloys. *J. Alloy. Compd.* **2013**, *578*, 373–379. [CrossRef]
46. Monogenov, A.N.; Marchenko, E.S.; Baigonakova, G.A.; Yasenchuk, Y.F.; Garin, A.S.; Volinsky, A.A. Improved mechanical properties of porous nitinol by aluminum alloying. *J. Alloy. Compd.* **2022**, *918*, 165617. [CrossRef]
47. Kaftaranova, M.; Hodorenko, V.; Anikeev, S.; Artyukhova, N.; Shabalina, A.V.; Gunther, V. Investigation of the Effect of Copper Addition on Physical and Mechanical Properties of TiNi-Cu Porous Alloy. *Metals* **2022**, *12*, 1696. [CrossRef]
48. Sharma, A.K.; Singh, R.; Tiwari, A.K.; Sharma, A.K. Enhancement of Physical and Mechanical Characteristics of NiTi Composite Containing Ag and TiC. *J. Mater. Eng. Perform.* **2021**, *31*, 2934–2945. [CrossRef]
49. Anikeev, S.G.; Artyukhova, N.V.; Shabalina, A.V.; Kulinich, S.A.; Hodorenko, V.N.; Kaftaranova, M.I.; Promakhov, V.V.; Gunter, V.E. Preparation of porous TiNi-Ti alloy by diffusion sintering method and study of its composition, structure and martensitic transformations. *J. Alloy. Compd.* **2022**, *900*, 163559. [CrossRef]
50. Abidi, I.H.; Khalid, F.A.; Farooq, M.U.; Hussain, M.A.; Maqbool, A. Tailoring the pore morphology of porous nitinol with suitable mechanical properties for biomedical applications. *Mater. Lett.* **2015**, *154*, 17–20. [CrossRef]
51. Mehrabi, R.; Kadkhodaei, M. 3D phenomenological constitutive modeling of shape memory alloys based on microplane theory. *Smart Mater. Struct.* **2013**, *22*, 025017. [CrossRef]
52. Shariat, B.S.; Bakhtiari, S.; Yang, H.; Liu, Y. Controlled initiation and propagation of stress-induced martensitic transformation in functionally graded NiTi. *J. Alloy. Compd.* **2021**, *851*, 156103. [CrossRef]
53. Chen, W.; Yang, Q.; Huang, S.; Kruzic, J.J.; Li, X. Compression Behavior of Graded NiTi Gyroid-Structures Fabricated by Laser Powder Bed Fusion Additive Manufacturing Under Monotonic and Cyclic Loading. *Jom* **2021**, *73*, 4154–4165. [CrossRef]
54. Taheri Andani, M.; Haberland, C.; Walker, J.M.; Karamooz, M.; Sadi Turabi, A.; Saedi, S.; Rahmanian, R.; Karaca, H.; Dean, D.; Kadkhodaei, M.; et al. Achieving biocompatible stiffness in NiTi through additive manufacturing. *J. Intell. Mater. Syst. Struct.* **2016**, *27*, 2661–2671. [CrossRef]

55. Liu, B.; Pan, Y. Effect of Pore Shape on Mechanical Properties of Porous Shape Memory Alloy. *Micromachines* **2022**, *13*, 566. [CrossRef]
56. Galimzyanov, B.N.; Mokshin, A.V. Mechanical response of mesoporous amorphous NiTi alloy to external deformations. *Int. J. Solids Struct.* **2021**, *224*, 111047. [CrossRef]
57. Zhu, P.; Stebner, A.P.; Catherine Brinson, L. Plastic and transformation interactions of pores in shape memory alloy plates. *Smart Mater. Struct.* **2014**, *23*, 104008. [CrossRef]
58. Ravari, M.R.K.; Esfahani, S.N.; Andani, M.T.; Kadkhodaei, M.; Ghaei, A.; Karaca, H.; Elahinia, M. On the effects of geometry, defects, and material asymmetry on the mechanical response of shape memory alloy cellular lattice structures. *Smart Mater. Struct.* **2016**, *25*, 025008. [CrossRef]
59. Machado, G.; Louche, H.; Alonso, T.; Favier, D. Superelastic cellular NiTi tube-based materials: Fabrication, experiments and modeling. *Mater. Des.* **2015**, *65*, 212–220. [CrossRef]
60. Burr, A.; Persenot, T.; Doutre, P.-T.; Buffiere, J.-Y.; Lhuissier, P.; Martin, G.; Dendievel, R. A numerical framework to predict the fatigue life of lattice structures built by additive manufacturing. *Int. J. Fatigue* **2020**, *139*, 105769. [CrossRef]
61. Lu, X.; Wang, C.; Li, G.; Liu, Y.; Zhu, X.; Tu, S. The Mechanical Behavior and Martensitic Transformation of Porous NiTi Alloys Based on Geometrical Reconstruction. *Int. J. Appl. Mech.* **2017**, *9*, 1750038. [CrossRef]
62. Bagheri, A.; Yadollahi, A.; Mahtabi, M.J.; Paudel, Y.; Vance, E.; Shamsaei, N.; Horstemeyer, M.F. Microstructure-Based MultiStage Fatigue Modeling of NiTi Alloy Fabricated via Direct Energy Deposition (DED). *J. Mater. Eng. Perform.* **2022**, *31*, 4761–4775. [CrossRef]
63. Resnina, N.; Belayev, S.; Voronkov, A. Influence of chemical composition and pre-heating temperature on the structure and martensitic transformation in porous TiNi-based shape memory alloys, produced by self-propagating high-temperature synthesis. *Intermetallics* **2013**, *32*, 81–89. [CrossRef]
64. Di Cocco, V.; Iacoviello, F.; Natali, S. Fatigue microstructural evolution in pseudo elastic NiTi alloy. *Procedia Struct. Integr.* **2016**, *2*, 1457–1464. [CrossRef]
65. Eskil, M. The effect of aging temperature on transformation parameters of porous NiTi shape memory alloy fabricated by SHS. *Russ. J. Non-Ferr. Met.* **2013**, *54*, 104–111. [CrossRef]
66. Shariat, B.S.; Liu, Y.; Rio, G. Pseudoelastic behaviour of perforated NiTi shape memory plates under tension. *Intermetallics* **2014**, *50*, 59–64. [CrossRef]
67. Xu, J.L.; Bao, L.Z.; Liu, A.H.; Jin, X.J.; Tong, Y.X.; Luo, J.M.; Zhong, Z.C.; Zheng, Y.F. Microstructure, mechanical properties and superelasticity of biomedical porous NiTi alloy prepared by microwave sintering. *Mater. Sci. Eng. C Mater. Biol. Appl.* **2015**, *46*, 387–393. [CrossRef]
68. Zhang, L.; Zhang, Y.Q.; Jiang, Y.H.; Zhou, R. Superelastic behaviors of biomedical porous NiTi alloy with high porosity and large pore size prepared by spark plasma sintering. *J. Alloy. Compd.* **2015**, *644*, 513–522. [CrossRef]
69. Zhang, L.; He, Z.Y.; Tan, J.; Zhang, Y.Q.; Stoica, M.; Prashanth, K.G.; Cordill, M.J.; Jiang, Y.H.; Zhou, R.; Eckert, J. Rapid fabrication of function-structure-integrated NiTi alloys: Towards a combination of excellent superelasticity and favorable bioactivity. *Intermetallics* **2017**, *82*, 1–13. [CrossRef]
70. Sergey, A.; Valentina, H.; Timofey, C.; Nadezhda, A.; Victor, G.; Anatoliy, P.; Ji-hoon, K.; Ji-soon, K. Evaluation of reversible shape memory effect in porous SHS TiNi-based compounds fabricated at various ignition temperature. *Mater. Res. Express* **2018**, *6*, aaf0d4. [CrossRef]
71. İpek Nakaş, G.; Dericioğlu, A.F.; Bor, Ş. Monotonic and cyclic compressive behavior of superelastic TiNi foams processed by sintering using magnesium space holder technique. *Mater. Sci. Eng. A* **2013**, *582*, 140–146. [CrossRef]
72. Dadbakhsh, S.; Speirs, M.; Kruth, J.-P.; Van Humbeeck, J. Influence of SLM on shape memory and compression behaviour of NiTi scaffolds. *CIRP Ann.* **2015**, *64*, 209–212. [CrossRef]
73. Taheri Andani, M.; Saedi, S.; Turabi, A.S.; Karamooz, M.R.; Haberland, C.; Karaca, H.E.; Elahinia, M. Mechanical and shape memory properties of porous Ni 50.1 Ti 49.9 alloys manufactured by selective laser melting. *J. Mech. Behav. Biomed. Mater.* **2017**, *68*, 224–231. [CrossRef] [PubMed]
74. Abdollahzadeh, M.; Hoseini, S.H.; Faroughi, S. Modeling of superelastic behavior of porous shape memory alloys. *Int. J. Mech. Mater. Des.* **2019**, *16*, 109–121. [CrossRef]
75. Gur, S.; Frantziskonis, G.N.; Muralidharan, K. Atomistic simulation of shape memory effect (SME) and superelasticity (SE) in nano-porous NiTi shape memory alloy (SMA). *Comput. Mater. Sci.* **2018**, *152*, 28–37. [CrossRef]
76. Jahadakbar, A.; Nematollahi, M.; Safaei, K.; Bayati, P.; Giri, G.; Dabbaghi, H.; Dean, D.; Elahinia, M. Design, Modeling, Additive Manufacturing, and Polishing of Stiffness-Modulated Porous Nitinol Bone Fixation Plates Followed by Thermomechanical and Composition Analysis. *Metals* **2020**, *10*, 151. [CrossRef]
77. Ravari, M.R.K.; Kadkhodaei, M.; Ghaei, A. A microplane constitutive model for shape memory alloys considering tension–compression asymmetry. *Smart Mater. Struct.* **2015**, *24*, 075016. [CrossRef]
78. Karamooz-Ravari, M.R.; Taheri Andani, M.; Kadkhodaei, M.; Saedi, S.; Karaca, H.; Elahinia, M. Modeling the cyclic shape memory and superelasticity of selective laser melting fabricated NiTi. *Int. J. Mech. Sci.* **2018**, *138–139*, 54–61. [CrossRef]
79. Zhu, X.; Chu, L.; Dui, G. Constitutive Modeling of Porous Shape Memory Alloys Using Gurson–Tvergaard–Needleman Model Under Isothermal Conditions. *Int. J. Appl. Mech.* **2020**, *12*, 2050038. [CrossRef]

80. Yu, Z.; Xin, R.; Xu, Z.; Sha, L.; Chen, L.; Zhu, Y.; Liang, P.; Zhang, Z.; Liu, Z.; Cao, Q. Shock-Resistant and Energy-Absorbing Properties of Bionic NiTi Lattice Structure Manufactured by SLM. *J. Bionic Eng.* **2022**, *19*, 1684–1698. [CrossRef]
81. Ma, C.; Gu, D.; Dai, D.; Yang, J.; Zhang, H.; Guo, M.; Wang, R.; Gao, J.; Chen, W.; Song, Y. Tailored pore canal characteristics and compressive deformation behavior of bionic porous NiTi shape memory alloy prepared by selective laser melting. *Smart Mater. Struct.* **2020**, *29*, ab9399. [CrossRef]
82. Schryvers, N.; Volkov, A.E.; Evard, M.E.; Iaparova, E.N.; Van Humbeeck, J. Modeling of Functional Properties of Porous Shape Memory Alloy. *MATEC Web Conf.* **2015**, *33*, 02006. [CrossRef]
83. Shariat, B.S.; Liu, Y.; Rio, G. Numerical modelling of pseudoelastic behaviour of NiTi porous plates. *J. Intell. Mater. Syst. Struct.* **2013**, *25*, 1445–1455. [CrossRef]
84. Shariat, B.S.; Liu, Y.; Rio, G. Finite element computational modelling and experimental investigation of perforated NiTi plates under tension. *Mater. Res. Bull.* **2013**, *48*, 5099–5104. [CrossRef]
85. Maîtrejean, G.; Terriault, P.; Brailovski, V. Density dependence of the superelastic behavior of porous shape memory alloys: Representative Volume Element and scaling relation approaches. *Comput. Mater. Sci.* **2013**, *77*, 93–101. [CrossRef]
86. Wu, Z.; Liu, B.; Wei, J.; Yang, Y.; Zhang, X.; Deng, J. Design of Porous Shape Memory Alloys with Small Mechanical Hysteresis. *Crystals* **2022**, *13*, 34. [CrossRef]
87. Ibrahim, H.; Jahadakbar, A.; Dehghan, A.; Moghaddam, N.; Amerinatanzi, A.; Elahinia, M. In Vitro Corrosion Assessment of Additively Manufactured Porous NiTi Structures for Bone Fixation Applications. *Metals* **2018**, *8*, 164. [CrossRef]
88. Zhou, D.; Gao, Y.; Lai, M.; Li, H.; Yuan, B.; Zhu, M. Fabrication of NiTi Shape Memory Alloys with Graded Porosity to Imitate Human Long-bone Structure. *J. Bionic Eng.* **2015**, *12*, 575–582. [CrossRef]
89. Zhang, X.; Yang, F.; Liu, B.; Deng, J. Design of Menger sponge fractal structural NiTi as bone implants. *Model. Simul. Mater. Sci. Eng.* **2021**, *29*, ac2b03. [CrossRef]
90. Lu, H.Z.; Ma, H.W.; Luo, X.; Wang, Y.; Wang, J.; Lupoi, R.; Yin, S.; Yang, C. Microstructure, shape memory properties, and in vitro biocompatibility of porous NiTi scaffolds fabricated via selective laser melting. *J. Mater. Res. Technol.* **2021**, *15*, 6797–6812. [CrossRef]
91. Jian, Y.T.; Yang, Y.; Tian, T.; Stanford, C.; Zhang, X.P.; Zhao, K. Effect of Pore Size and Porosity on the Biomechanical Properties and Cytocompatibility of Porous NiTi Alloys. *PLoS ONE* **2015**, *10*, e0128138. [CrossRef]
92. Liu, X.; Wu, S.; Yeung, K.W.; Chan, Y.L.; Hu, T.; Xu, Z.; Liu, X.; Chung, J.C.; Cheung, K.M.; Chu, P.K. Relationship between osseointegration and superelastic biomechanics in porous NiTi scaffolds. *Biomaterials* **2011**, *32*, 330–338. [CrossRef] [PubMed]
93. Sharma, N.; Raj, T.; Kumar, K. Physical and tribological characteristics of porous NiTi SMA fabricated by powder metallurgy. *Part. Sci. Technol.* **2016**, *35*, 541–546. [CrossRef]
94. Zhang, X.X.; Hou, H.W.; Wei, L.S.; Chen, Z.X.; Wei, W.T.; Geng, L. High damping capacity in porous NiTi alloy with bimodal pore architecture. *J. Alloy. Compd.* **2013**, *550*, 297–301. [CrossRef]
95. Kakaei, K.; Akbarpour, M.R.; Liyaghi, Z. Synthesis of partially oxidized NiTi nanostructure by high energy ball milling and its application to supercapacitor. *J. Mater. Sci. Mater. Electron.* **2017**, *29*, 2222–2227. [CrossRef]
96. Bewerse, C.; Emery, A.A.; Brinson, L.C.; Dunand, D.C. NiTi porous structure with 3D interconnected microchannels using steel wire spaceholders. *Mater. Sci. Eng. A* **2015**, *634*, 153–160. [CrossRef]

Disclaimer/Publisher's Note: The statements, opinions and data contained in all publications are solely those of the individual author(s) and contributor(s) and not of MDPI and/or the editor(s). MDPI and/or the editor(s) disclaim responsibility for any injury to people or property resulting from any ideas, methods, instructions or products referred to in the content.